Received: 10 December 2020 | Revised: 22 February 2021 | Accepted: 3 April 2021
DOI: 10.1002/ar.24692

SPECIAL ISSUE ARTICLE

The Anatomical Record
WILEY

The functional morphology of the postpulmonary septum of the American alligator (*Alligator mississippiensis*)

Michael Cramberg | **Skye Greer** | **Bruce A. Young**

Department of Anatomy, Kirksville College of Osteopathic Medicine, AT Still University, Kirksville, Missouri

Correspondence
Bruce A. Young, Department of Anatomy, Kirksville College of Osteopathic Medicine, AT Still University,
800 W. Jefferson Street, Kirksville, Missouri, 63501, USA.
Email: byoung@atsu.edu

Abstract

The American alligator (*Alligator mississippiensis*) has a postpulmonary septum (PPS) that partitions the intracoelomic cavity. The PPS adheres to the capsule of the liver caudally and to the visceral pleura of the lung cranially; the ventrolateral portions of the PPS are invested with smooth muscle, the remainder is tendinous. Differential pressure transducers were used to record the intrathoracic (ITP) and intraperitoneal (IPP) pressures, and determine the transdiaphragmatic pressure (TDP). Each ventilatory pulse resulted in a pulse in ITP and a significantly lower pulse in IPP; meaning that a TDP was established, and that the pleural and peritoneal cavities were functionally isolated. The anesthetized alligators were tilted 30° head-up or head-down in order to displace the liver. Head-up rotations caused a significant increase in IPP, and a significant decrease in ITP (which became negative); head-down rotations produced the opposite effect. During these rotations, the PPS maintained opposite pressures (positive or negative) in the pleural and peritoneal cavities, and established TDPs greater than have been reported for some mammals. Two types of "breaths" were recorded during these experiments. The first was interpreted as a contraction of the diaphragmaticus muscle, which displaces the liver caudally; these breaths had the same effect as the head-up rotations. The second type of breath was interpreted as constriction of the thoracic and abdominal body walls; this type of breath produced pronounced, long-duration, roughly parallel, increases in ITP and IPP. The smooth muscle within the PPS is suggestive of higher-order adjustment or tuning of the PPS's tensile state.

KEYWORDS

hepatic pump, intraperitoneal, intrathoracic, reptile, transdiaphragmatic pressure, ventilation

1 | INTRODUCTION

The diaphragm of mammals is a morphological composite with a central tendon of collagen fibers and a periphery of skeletal muscle; there is considerable variation in the exact relationship of these two components within mammals (Perry, Similowski, Klein, & Codd, 2010). The mammalian diaphragm can function in ventilation, since contraction of the diaphragm's skeletal muscle increases the volume of the pleural cavity, creating negative intrathoracic pressure, expansion of the lungs, and inhalatory airflow (Lessa, de Abreu, Bertassoli, & Ambrosio, 2016).

In mammals the diaphragm also functions to separate the slightly negative (e.g., Agostoni & Rahn, 1960; Bishop, 1963) intrathoracic pressure (ITP) from the slightly positive (e.g., Pelosi, Quintel, & Malbrain, 2007; Sanchez et al., 2001) intraperitoneal pressure (IPP). The difference between the pressures in these two body cavities is referred to as the transdiaphragmatic pressure, or TDP. In mammals, the TDP can be influenced by body posture (Hodges, Butler, McKenzie, & Gandevia, 1997), and by a number of acute and chronic physiological states or conditions (Hubmayr, Sprung, & Nelson, 1990). Recent work on cetaceans (Lillie et al., 2017) has highlighted the influence that external pressures can have on transdiaphragmatic pressure.

In reptiles, the "pleural" and "peritoneal" cavities are often continuous, though in turtles, crocodilians, and some squamate reptiles the body cavity is at least partially separated by a structure commonly termed the postpulmonary septum or PPS (Butler, 1889; Duncker, 1979; Klein & Owerkowicz, 2006; Lyson et al., 2014). The PPS differs significantly among reptiles, particularly in the presence, or absence, of either smooth or skeletal muscle within the septum (George & Shah, 1954; Klein & Owerkowicz, 2006). The crocodilian PPS has been described in detail (see Duncker, 1978a, 1978b), and was more recently detailed by Van der Merwe and Kotze (1993). Mushonga and Horowitz (1996) detailed the connections between the PPS and the adjacent soft tissue structures, particularly bursae. More recent work has explored the functional role of another reptilian intracoelomic septum, the posthepatic septum, in teid lizards (Klein, Abe, & Perry, 2003; Klein, Andrade, Abe, & Perry, 2003a, 2003b; Klein, Bohme, & Perry, 2000). To date nothing is known about the functional performance of the PPS in Crocodylians.

Crocodylians have some of the most variable ventilatory mechanics of any vertebrate (see Brocklehurst, Schachner, Codd, & Sellers, 2020 for a recent review). They are capable of episodic breathing (Douse & Mitchell, 1992; Milsom, 1991) with long periods of apnea and voluntary redistribution of blood away from the pulmonary circuit (Axelsson, Franklin, Lofman, Nilsson, & Grigg, 1996; Syme, Gamperl, & Jones, 2002). When they are ventilating, inhalatory airflow can be achieved in a number of ways including expansion of the thoracic ribs (Brocklehurst, Moritz, Codd, Sellers, & Brainerd, 2017; Claessens, 2009), active caudal displacement of the liver (Gans & Clark, 1976; Munns, Owerkowicz, Andrewartha, & Frappell, 2012; Uriona & Farmer, 2006), or expansion of the abdominal body wall, potentially including displacement of the pelvis (Farmer & Carrier, 2000a). Crocodylians can perform one or more of these inhalatory mechanics at the same time, and can readily switch between modes (Farmer & Carrier, 2000b; Klassen, Adams, Cramberg, Knoche, & Young, 2020). Complicating this further is the inter- and intra-specific diversity among Crocodylians; some forms use the active displacement of the liver as a form of buoyancy control (Uriona & Farmer, 2008), can adopt a more regular ventilatory pattern during sustained terrestrial locomotion (Farmer & Carrier, 2000b), and there are scaling changes to the Crocodylian body wall compliance (Reichert et al., 2019). Despite the numerous studies that have been done on the ventilatory mechanics of Crocodylians, no experimental work has been done on the PPS. In fact, some of the published studies on Crocodylian ventilatory mechanics never mention the PPS (e.g., Reichert et al., 2019).

The purpose of this study was to examine the PPS of the American alligator (*Alligator mississippiensis*) using some of the same techniques that have been applied to the mammalian diaphragm. The focus of this study is not on the ventilatory mechanics of *A. mississippiensis*, but rather on the dynamics of the PPS in this species. The findings presented herein demonstrate that the PPS of *A. mississippiensis* functional segregates the pleural and peritoneal cavities, is capable of maintaining transdiaphragmatic pressures similar to those reported from some mammals, and depends on a dynamic tension that can be modulated by the animal. For all of these reasons, and others presented in the discussion, we will argue that the postpulmonary septum of *A. mississippiensis* should be considered a diaphragm.

2 | MATERIALS AND METHODS

2.1 | Live animals

Six live sub-adult (143–188 cm total length, 7.9–23.1 kg mass) American alligators (*Alligator mississippiensis*) were obtained from the Louisiana Department of Wildlife and Fisheries. The animals were housed communally in a 29 m^2 facility that featured three submerging ponds, natural light, and artificial lights on a 12:12 cycle. The facility was maintained at 30–33° C. Warm water rain showers were provided every 20 min, which helped maintain the facility at >75% relative humidity. The alligators were maintained on a diet of previously frozen adult rats. When individual animals were removed from the enclosure, they were caught by noosing, induced to bite a bite pad, then their jaws taped shut around the bite pad using vinyl tape. The husbandry and use of the live alligators followed all applicable federal guidelines, and were approved by the IACUC of A.T. Still University (Protocol #217, approved March 22, 2020).

2.2 | Morphology

The diaphragm and surrounding tissues were imaged using a number of live alligators. One alligator was positioned under a veterinary radiograph (Digital Portable X-Ray Unit, Bowie) and imaged at 70 kv and 20 mA for 0.25 s. Three specimens, restrained only by tape around the jaws and limbs, were placed prone within a phased-array surface coil that was centered around their PPS. When calm, the alligator was imaged with a clinical 0.35-T MRI unit (Ovation, GE Medical Systems, Milwakee, Wisconsin; Sagittal T1-weighted 3D fast spoiled gradient, 11.5/4.9, flip angle 30°, field of view 300 mm, slice 10 mm, matrix 192 × 160, Nex 2, scan time 1 min 4 s). One alligator was lightly anesthetized with Isoflurane then placed within a clinical 64-detector CT unit (Ingenuity, Philips Medical, Einthoven, the Netherlands). Images were captured through helical acquisition at 0.67 mm, FOV 160 mm, 100 kV, 125 mAs, with a rotation time of 500 msec, section thickness of 0.67 mm, and pitch of 0.391. Images were reconstructed coronally and sagittally, then digitally manipulated (using the Philips Ingenuity software) to remove portions of the body wall and heart.

The PPS and surrounding tissues were dissected from previously preserved (in neutral-buffered formalin or NBF) 160 and 175 cm total length specimens of *Alligator mississippiensis* in the private collection of Prof. Young. Additional dissections were performed on freshly euthanized sub-adult specimens. Portions of the PPS were excised, then dehydrated through an ethanol series prior to paraffin embedding. Transverse and frontal sections were cut at 10 μm. The initial classification of the tissues within the PPS was based on morphological features and the staining response to Hematoxylin and Eosin, Van Gieson's stain, and Masson's trichrome stain. Additional staining protocols intended to identify skeletal muscle (Verhoff's Iron Hematoxylin and Rapid PTAH stain) were also performed. Additional gross and histological analyses were performed on three NBF preserved hatchling specimens (26–29 cm) of *A. mississippiensis* from the collection of Prof. Young. Microscopic anatomy was documented using a DM 4000B microscope (Leica Microsystems Inc., Buffalo Grove, IL).

2.3 | Pressure recordings

Each individual alligator was placed on a stiff board (244 × 28 × 3.8 cm thick), which exceeded the maximum width and length of the alligators used for this study. Six 2.5 cm wide heavy duty straps (Northwest Tarp and Canvas; Bellingham, WA) were used to secure the alligator to the board; the straps were tight enough to minimize movement of the animal but not tight enough to impede ventilation or circulation.

With the alligator's mouth held open by the bite pad, a laryngoscope was used to depress the gular valve and expose the glottis. A cuffed endotracheal tube was inserted into the larynx and connected to a custom anesthesia system that included a ventilator pump (Harvard), Vaporstick anesthesia machine (Surgivet), Isoflurane vaporizer (Surgivet), and Capnomac Ultima respiratory gas monitor (Datex-Engstrom). The alligators were maintained on a steady ventilatory pattern of 8 breaths per minute each with a tidal volume of 500 ml. Anesthesia was accomplished using 5% Isoflurane. Once the alligator was fully anesthetized, the straps were re-arranged so that the head and neck were secure, as was the pelvis and tail, but no straps were on the alligator's trunk. To further immobilize the animal, the limbs were restrained against the board in an extended position.

Two small incisions were made in the dorsolateral scalation, one cranial to, and the other caudal to, the diaphragm. Through these incisions the dorso-lateral body wall of the peritoneum and the intercostal musculature of the thorax were exposed; a small surgical opening was made in the outer layers of both portions of the body wall. Two differential pressure transducers (DLP25, Harvard Apparatus) were mounted over the alligator's body. Approximately 4 cm length of (3.2 mm I.D.) tubing connected each transducer's input port to a 3.2 mm O.D. hypodermic needle; both ends of the tubing were sealed with epoxy glue. The needle tip and approximately 2 cm of the needle shaft extended free of the tubing. The free tip of the hypodermic needle was passed through the surgical opening such that the needle entered either the pleural cavity or the peritoneal cavity. The outer surface of the needle, and the adjacent incision, were covered with petroleum jelly to ensure a pressure seal at the body wall.

The pressure transducers were coupled to strain gauge amplifiers (P122, GRASS Instruments). The outputs from these two amplifiers were sampled at 2 kHz, simultaneously with the exhalatory CO_2 record from the respiratory gas monitor, using the MiDas data acquisition system (Xcitex). After the surgeries, the differential pressure transducers were calibrated using a small animal pressure monitor and limiter (HSE-HA, Harvard Apparatus).

2.4 | Experimental design

This study was not designed to examine ventilation in *Alligator mississippiensis*, or the pattern of airflow through the alligator lung. The goal of this study was to document the functional properties and plasticity of the PPS of *Alligator*. To address this, three different data sets were collected:

1. Pulmonary Inflation: Using the ventilator, a fixed amount of gas was forced into the alligator lung at a fixed interval (8 breaths per minute, or 0.13 Hz). The pulse presented to the lung was designed to be just enough to keep the animal alive and anesthetized. The goal was to produce slight expansion of the lung in the pleural cavity, but minimal or no displacement of the alligator's body wall. The pulmonary inflation data were only collected while the animal was horizontal.
2. Visceral displacement: The board that the alligators were positioned on was attached to a spindle that had machine stops at 30° above and below the horizontal. With the head and tail of the anesthetized alligator fixed as described above, the table could be quickly rotated without causing any displacement of the alligator. These tilts were intended to cause a displacement of the alligator's viscera, particularly the liver, with minimal to no displacement of the animal's body wall.
3. "Breaths": These were lengthy experiments, typically lasting 10–12 hr. During this time, the alligators were maintained at a surgical plane of anesthesia. None of the animals recovered from anesthesia during the experiments. However, occasional movements of the alligator's thoracic and/or abdominal body wall were observed visually and recorded. For simplicity, these movements will hereafter be described as "breaths." These intermittent movements of the body wall resembled what were observed from the alligator during normal ventilation prior to anesthesia. Nevertheless, we cannot exclude the possibility that these movements were reflexive responses to the surgical manipulation of the body wall, the induced movement of the viscera, or the presence of the needles. Accordingly, the use of the term "breath" is not meant to imply that these alligators had recovered from anesthesia and were consciously ventilating. In order to consider an episode a "breath" three conditions had to be met: (a) pressure changes had to be observed in both body cavities; (b) these changes had to occur independent of any form of stimulation, contact, or alteration of the alligator; and (c) the pressure changes had to produce some alteration of the simultaneously recorded CO_2 trace (Figure 1). The last criterion was the most variable, since the temporal pattern of the breaths was independent of the (fixed) ventilatory cycle.

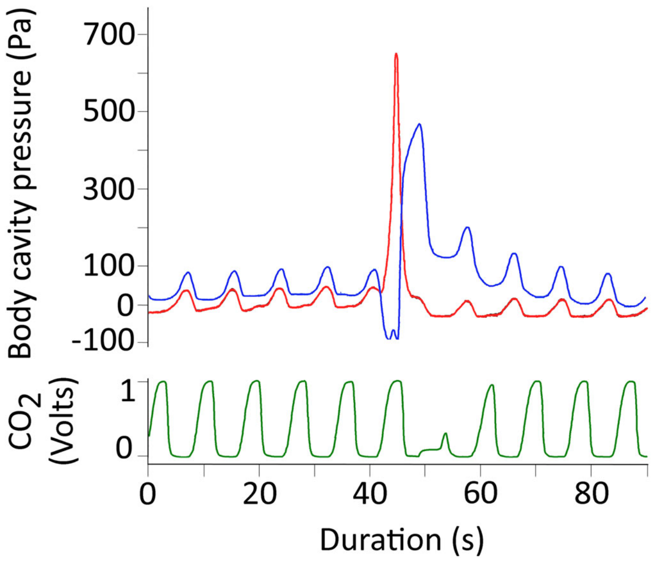

FIGURE 1 Raw data traces simultaneously recorded from a 152 cm *Alligator mississippiensis*. When these traces were recorded the anesthetized alligator was horizontal, and was not contacted or stimulated in any way. The prominent shifts in IPP (red) and ITP (blue) are what are herein referred to as a "breath." Note that the exhalatory CO_2 trace (green) which was recorded during stable ventilation was altered by the pressure changes in the body cavities

The changes in ITP and IPP associated with the alligator's breaths were difficult to record. The temporal duration, particularly of the synchronous breaths (see below) were such that often only a portion of the breath was recorded in the 90 s data window. There was always a concern that these breaths were an indication that the alligator was starting to recover from anesthesia. Though no other evidence of recovery was ever noted, ethically the experiments could not be extended purely in an attempt to record additional breaths. Lastly, only breaths that occurred during baseline (horizontal) recordings were quantified. It was not possible to isolate the pressure changes caused by tilting the alligator from those caused by a breath.

2.5 | Data analysis

Using the MiDas software, the amplitudes of the intrathoracic pressure (ITP) and intraperitoneal pressure (IPP) curves were quantified for each pulse. Data were always taken from simultaneously recorded ITP and IPP pulses; to minimize bias no more than three pulses were quantified from each 90s data trace. For the purpose of this study transdiaphragmatic pressure will be defined as ITP-IPP, and the transdiaphragmatic ratio as ITP/IPP. Traces of ITP and IPP pulsations were imported into SpectraPlus (Pioneer Hill Software) for FFT and Power Spectrum analysis (with 32,768 points, a Hanning window, and a spectral resolution of 0.065 Hz).

This study relied on large diameter needles, just the tips of which were passed through the parietal pleura or parietal peritoneum; the needles were always located in the dorso-lateral portion of the body cavity, on either side of the hepatopulmonary bursae. For this to work the needles had to project far enough that they would remain in patent contact with the body cavity despite any visceral shifts, they had to be fixed relative to the body wall and the respective lining serosa, and they could not project far enough into the cavities to interfere with any visceral displacement. Meeting these conditions was difficult, particularly while tilting the animals or during periods of ventalatory-induced body wall displacement. Often under these conditions, one or both pressure tracings would be lost (Figure 2). All trials in which either pressure tracing was lost were excluded from analysis; all trials in which both pressure tracings were maintained were fully included in the analysis. The amplitudes of individual pulses were compared using ANOVA to document any intra-specific variation. The visceral displacement trials and the "breaths" were intended to document changes in the ITP and IPP; accordingly, these data sets were pooled across the alligators and compared using paired *t* tests.

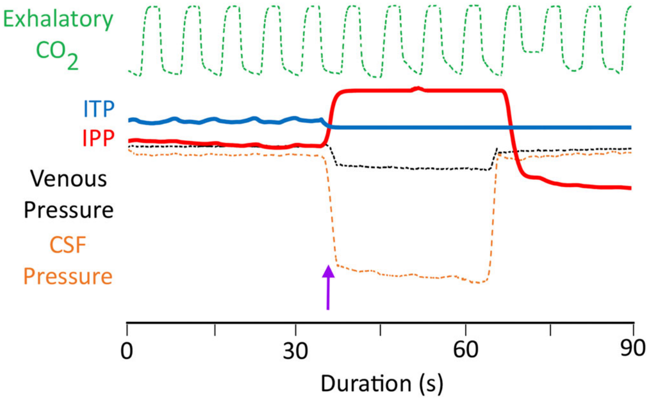

FIGURE 2 Example of the loss of a pressure sensor trace. This figure shows raw simultaneously recorded data traces for exhalatory CO_2 (dashed green line), ITP (blue trace), IPP (red trace), as well as cerebrospinal fluid pressure (orange dashed line), and jugular venous pressure (dashed black line). Note that the CSF and venous pressures were recorded for a different study. When this 155 cm alligator was rotated to 30° head-up (purple arrow), the IPP, CSF, and venous pressure traces all responded. Following this rotation, the shift in the ITP trace was less than expected, there were no deflections in the ITP trace associated with ventilation, and the ITP trace remained constant when the animal was returned to horizontal (though all other variables shifted). Due to the lack of response from the ITP sensor, these data traces were excluded from the analysis

3 | RESULTS

3.1 | Morphology

The caudal border of the pleural cavity of *Alligator mississippiensis*, which can be aligned with the intervertebral joint between the 11th thoracic and the first lumbar vertebrae, is uneven and asymmetric (Figure 3a), and so is the course of the postpulmonary septum (PPS). Ventrally the pericardial sac forms the bulk of the mediastinum. Cranially, the pericardial sac is wedged between the two lungs, while caudally both lateral surfaces of the pericardial sac abut the liver (Figure 3b). The PPS is located between the lungs and liver, fusing to, and curving around, the pericardial sac (Figure 3b). The lateral portions of the PPS are more oblique, due to the lungs extending caudally over the liver in the dorsal, but not the ventral, portions of the body (Figure 3c). Both the lungs and the liver are absent from the sagittal midline, here the caudal surface of the pericardial sac is separated from the expansive stomach by the PPS (Figure 3d,e).

These spatial relationships can be seen in gross dissection. If the caudal thoracic and cranial lumbar vertebrae are removed, the nearly perpendicular relationship between the dorsal mediastinum and the PPS is exposed (Figure 4a). If the lungs are partially or fully excised, the PPS can be seen forming the caudal wall of the pleural cavity (Figure 4b). The pericardial sac can be seen in the caudoventral portion of the mediastinum, between the two lungs (Figure 4); the PPS in this region is thin and tendinous, it fuses to the outer surface of the fibrous pericardium and courses along the caudal surface of the pericardial sac. There are small portals present in the dorsolateral portions of the PPS (Figure 4b), these lead into small caudal extensions of the pleural cavity which have been termed the hepatopulmonary bursae (Mushonga & Horowitz, 1996).

The PPS has three attachments which are critical to its functional performance (Figure 5). The PPS is anchored to the inner surface of the body wall (Figure 5b), this attachment is more robust in the ventral portion of the PPS, but is present throughout the perimeter of the PPS. Collagen fibers on the caudal surface of the PPS integrate into the cranial surface of the collagenous capsule surrounding the liver (Figure 5c). There are also attachments between the collagen on the cranial surface of the PPS, and the connective tissue on the caudal surface of the lung (Figure 5d).

The diaphragmaticus muscle attaches to the posthepatic septum and to the capsule of the liver (Figure 6a, b). The attachments of the diaphragmaticus are prominent on the caudal portion of the liver. The postpulmonary septum can be dissected free of the liver

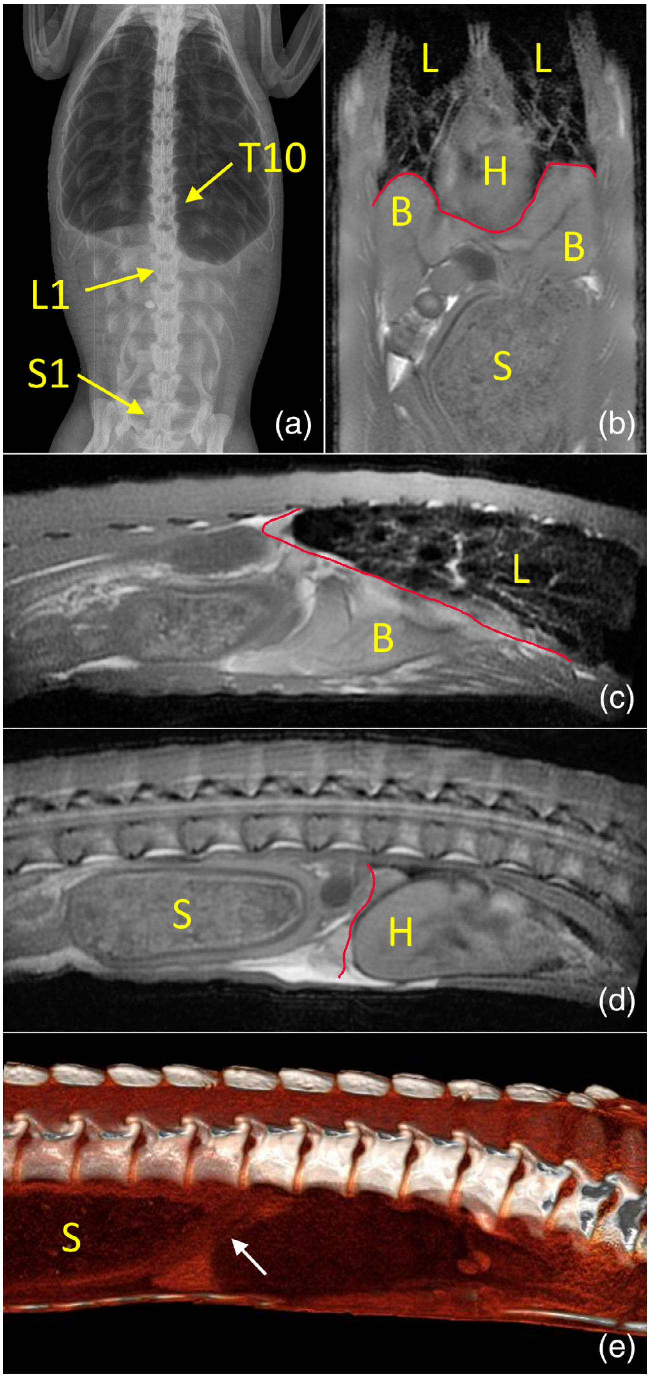

FIGURE 3 Anatomical position of the postpulmonary septum (red line) of *Alligator mississippiensis*. (a) radiograph showing the asymmetrical caudal extant of the lungs, some of the vertebrae have been numbered for reference; (b) frontal plane MRI taken near the abdominal surface; (c) parasagittal MRI taken near the lateral body wall; (d) sagittal MRI; (e) parasagittal CT similar to (d), in this image the body wall and heart have been digitally removed to highlight the course of the postpulmonary septum (arrow). B, liver; H, heart; L, lungs; S, stomach

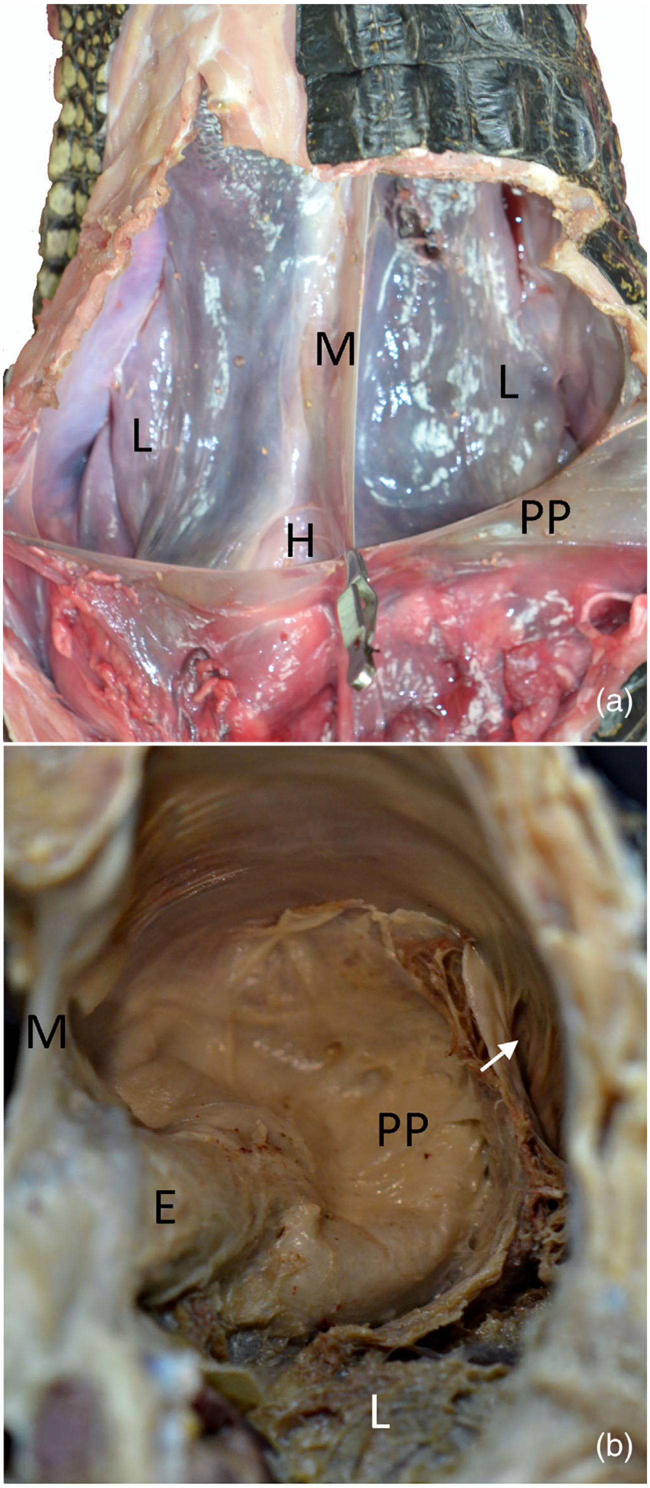

FIGURE 4 Gross morphology of the postpulmonary septum of *Alligator mississippiensis*. (a) dorsal view of the mediastinum and postpulmonary septum. (b) Apical (cranial) view of the thoracic cavity, the postpulmonary septum is intact, as is the small bursae on the dorsolateral margin of the postpulmonary septum (arrow). E, esophagus; H, heart; L, lungs; M, mediastinum; PP, postpulmonary septum

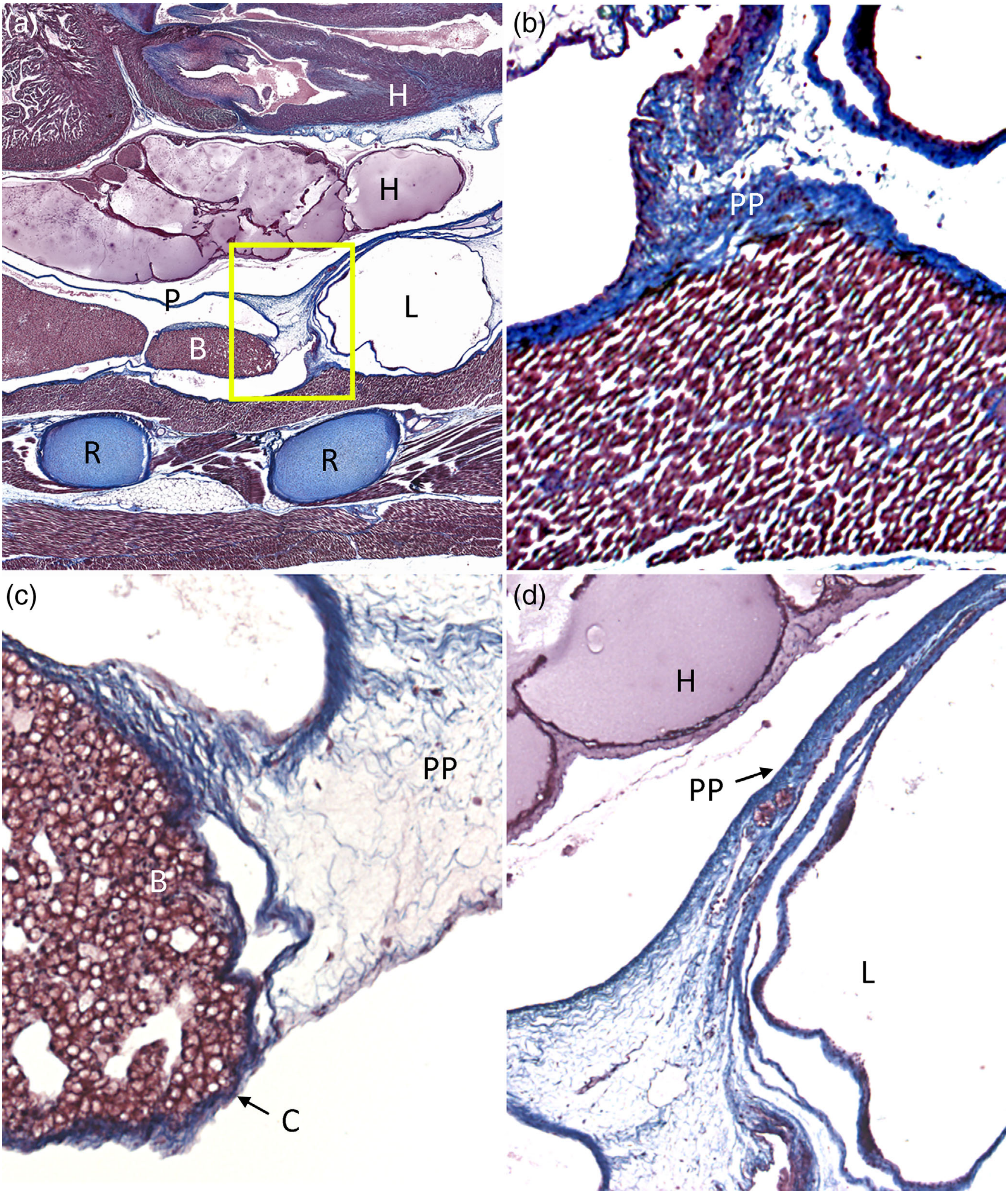

FIGURE 5 Attachments of the postpulmonary septum of *Alligator mississippiensis*. (a) frontal section through a hatchling specimen, showing the key morphological attachments of the postpulmonary septum; images B-D are highlights from within the yellow square; (b) the postpulmonary septum attached to the inner surface of the lateral body wall; (c) the postpulmonary septum fusing to the capsule of the liver along the cranial surface of the liver; (d) thickening of the postpulmonary septum as it courses along the caudal surface of the lung and fuses with the pericardium. B, liver; C, capsule of the liver; H, heart; L, lungs; P, pericardium; PP, postpulmonary septum; R, rib

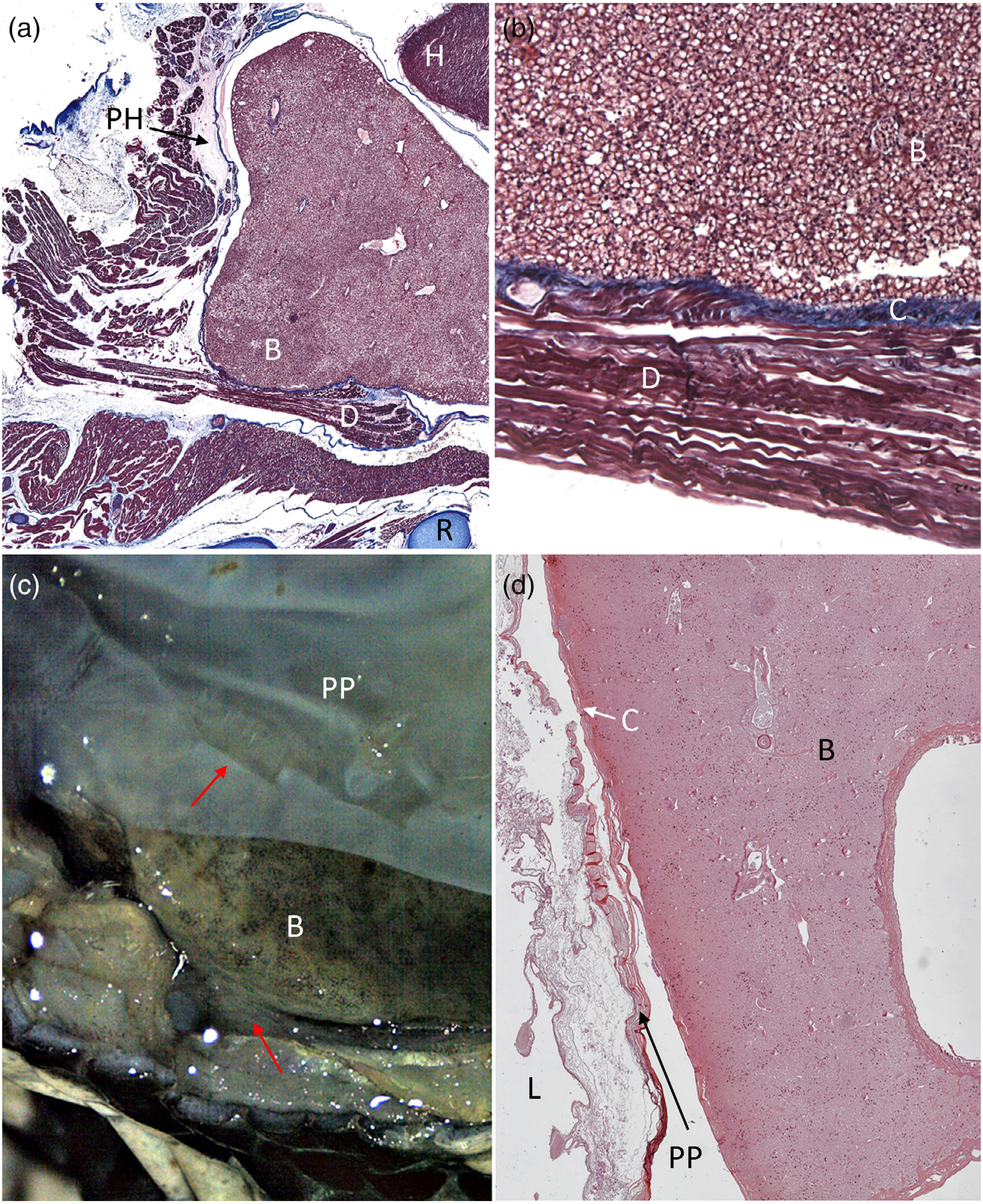

FIGURE 6 Morphology of *Alligator mississippiensis*. (a) frontal section through a hatchling showing the caudal surface of the liver and the associated diaphragmaticus muscle; (b) increased magnification of (a) showing the attachment of the diaphragmaticus onto the capsule of the liver; note the wrinkling of the fibers of the diaphragmaticus; (c) the postpulmonary septum of a hatchling specimen, the lateral portion of the postpulmonary septum has been incised (red arrows) to demonstrate the separation between the postpulmonary septum and the liver; (d) histological section showing the lung and liver with the postpulmonary septum between them, note that the collagen fibers of the postpulmonary septum are fused to the capsule of the liver, and there is no diaphragmaticus muscle evident. B, liver; C, capsule of the liver; D, diaphragmaticus; H, heart; L, lung; PH, posthepatic septum; PP, postpulmonary septum; R, rib

without disrupting the diaphragmaticus muscle (Figure 6c). Histological sections (Figures 5d and 6d) cut through the PPS, lung, and liver reveal the prominent capsule surrounding the liver, but no skeletal muscle fibers, or tendinous attachments separate from the capsule of the liver.

The composition of the PPS of *A. mississippiensis* is spatially variable. The middle and dorsal portions of the PPS are thinner, and consist of overlapping sheets of collagen fibers. The lateral and ventral portions of the PPS are thicker; when viewed grossly there are organized bands within the PPS and associated neurovascular bundles (Figure 7a). Histological examination of these regions of the PPS revealed a prominent core of smooth muscle surrounded by sheets of collagen fibers (Figure 7b). Transverse sections through this portion of the PPS reveal that the smooth muscle is well organized with a dominant medio-lateral orientation (Figure 7c). It should be noted that the tissue of the PPS was examined with a variety of traditional stains, as well as more specialized stains chosen to highlight skeletal muscle striations (Verhoff's Iron hematoxylin and rapid PTAH stain). Each stain was applied to both the PPS and slides of known striated muscle from *Alligator*; all of the histological results indicate the PPS consists of smooth, not striated, muscle.

The spatial relationships of the structures being discussed are presented in Figure 8. The lungs have multiple septal connections to the PPS, and the caudal tip of the lung is typically fused to the cranial surface of the PPS. The PPS courses cranial to the capsule surrounding the liver; there are multiple points of adhesion/fusion between the two. The skeletal muscle of the diaphragmaticus inserts onto the capsule of the liver, it has no direct contact with the PPS. The posthepatic septum (PHS) is a thickening on the caudal portion of the capsule of the liver. This thickened connective tissue could be traced over the dorsal surface of the liver, but the contact between the PHS and the PPS in *A. mississippiensis* is no more pronounced than between the PPS and the capsule of the liver.

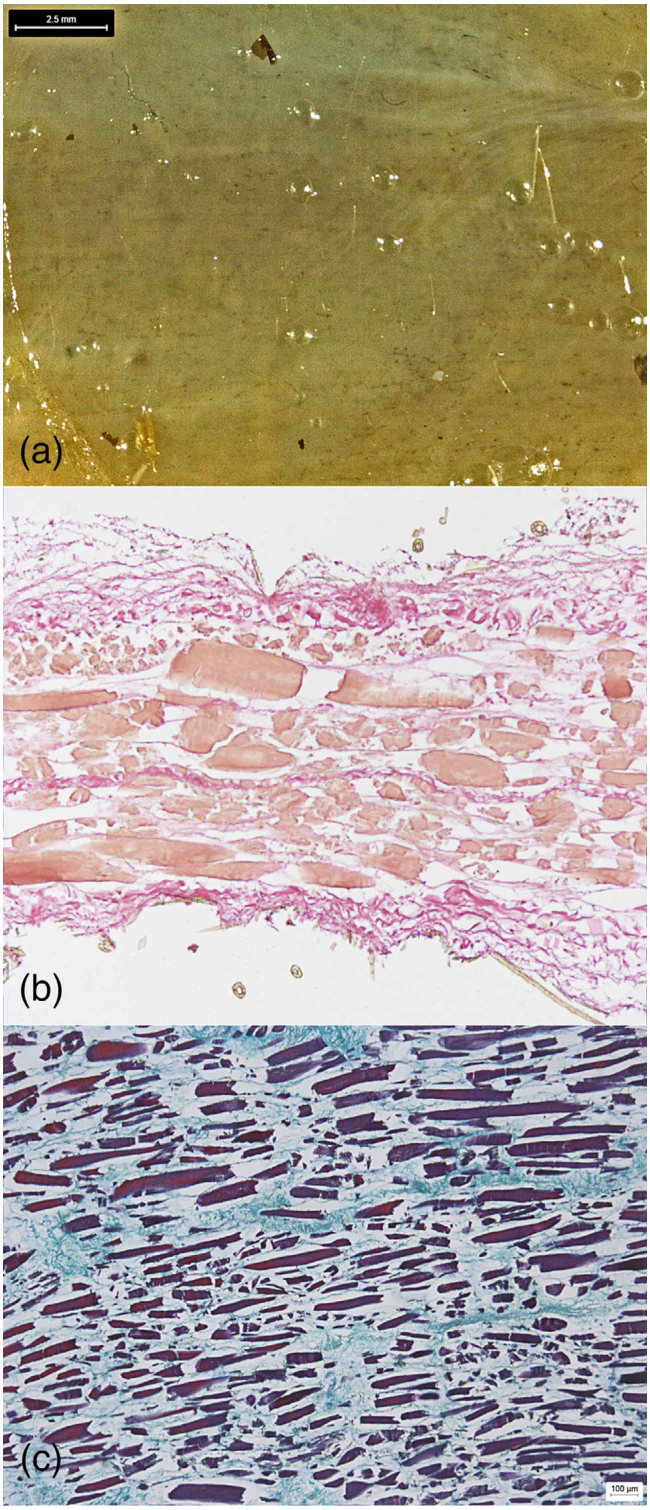

FIGURE 7 Structure of the postpulmonary septum of *Alligator mississippiensis*. (a) photograph of an excised portion of the postpulmonary septum showing bands of smooth muscle fibers and neurovascular bundles. (b) frontal section through the postpulmonary septum showing the prominent core of smooth muscle (stained salmon) surrounded by a periphery of collagen fibers (stained pink). (c) transverse section through the postpulmonary septum showing the similar (medio-lateral) orientation of the smooth muscle fibers (stained violet in this preparation)

3.2 | Pulmonary inflation

The anesthetized alligators, in a prone position with their body mass supported by a board, had mean resting intrathoracic pressures (ITP) of 725 Pa and mean resting intraperitoneal pressures (IPP) of −670 Pa. These resting values were recorded at first sensory implantation, during which the alligator was in apnea and had stabilized to no positive pressure ventilation. This study is primarily intended to examine the relative dynamics of the

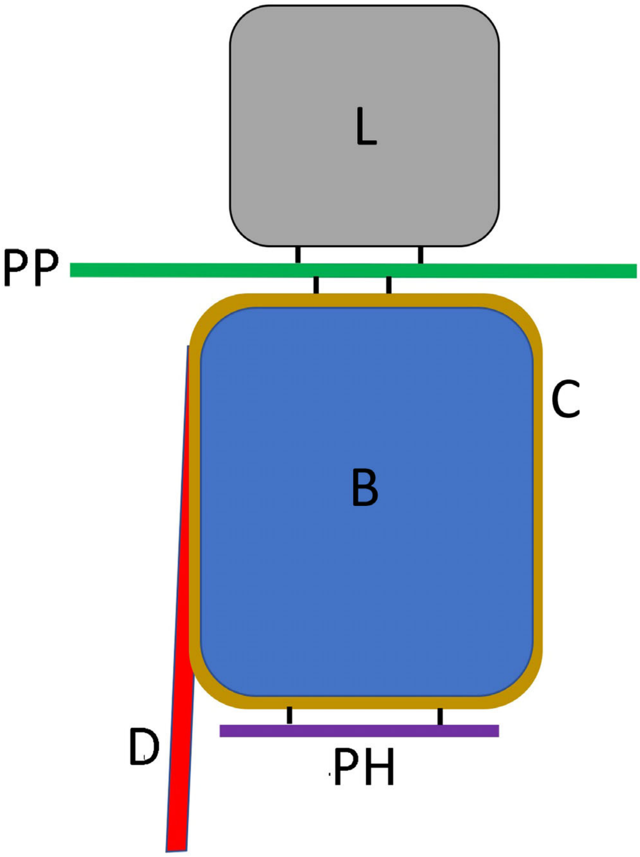

FIGURE 8 Simple schematic illustrating a dorsal perspective of the positional relationships of the postpulmonary septum. Though drawn separate for clarity, partially (or wholly) fused structures are indicated by the linking black lines. B, liver; C, capsule of the liver; D, diaphragmaticus; L, lungs; PH, posthepatic septum; PP, postpulmonary septum

postpulmonary septum; to better focus on this, the ITP and IPP traces were all adjusted (away from the resting pressures) to a starting level of 0 Pa.

The pulses of air the ventilator introduced into the alligator's trachea were sufficient to expand the lung, thereby altering the ITP. The resulting ITP pulsations tracked the ventilatory cycle and were associated with IPP pulsations (Figure 9). Simultaneously recorded ITP and IPP traces had similar Power Spectra (Figure 10). In all of the pulsations examined the dominant frequency (0.13 Hz) corresponded to the ventilation frequency, and the same series of harmonics were recorded on either side of the PPS (Figure 10).

In all of the alligators the mean ITP was greater than the mean IPP, though this difference was not significant for the 16.3 kg animal (Table 1). ANOVA revealed significant ($F = 97.76$, $p = 1.1^{-16}$, $N = 6$) differences in ITP among the alligators. Post-hoc Bonferroni analysis revealed that differences largely fell out according to the mass of the alligators; the smallest alligators (which had the highest ITP) were not significantly different from each other, but they were significantly different from the larger alligators (which had the lowest ITP). A similar pattern was found in the IPP data, which also had significant differences (ANOVA; $F = 55.23$, $p = 1.1^{-16}$, $N = 6$). Post-hoc Bonferroni analysis of the IPP data revealed that the smallest alligators, where the IPP was highest, were not significantly different from each other, but they were significantly different from the larger alligators, where the IPP was lowest (Table 1).

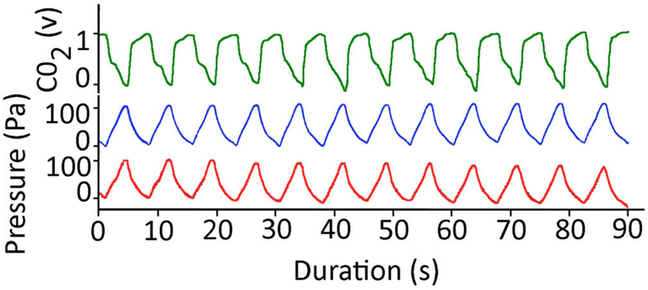

FIGURE 9 Raw data tracing showing 90 s of simultaneously recorded exhalatory CO_2 (green, upper trace), intrathoracic pressure (blue, middle trace), and intraperitoneal pressure (red, lower trace) from a 155 cm *Alligator mississippiensis*

These differences stem, at least in part, from the methodology employed. As noted above, the experimental design called for the ventilatory pulses to be held constant. As the alligators increased in mass, the scaling of their lungs and pleural cavities ensured that the same ventilatory pulse resulted in less ITP (Figure 11). The experimental design did not anticipate as much variation in body size among the study alligators. The experience with the smaller alligators (and larger specimens used for earlier surgical experiments) suggested that the 23 kg alligator might be at risk if maintained on the same ventilatory pulses used on the other alligators. Accordingly, the pressure for the largest alligator was increased, resulting in increased levels of ITP and IPP (Table 1 and Figure 11), as well as stable anesthesia.

The transdiaphragmatic pressures were positive, and of relatively low magnitude (Table 1). If the transdiaphragmatic pressures were pooled across the six alligators, there was a mean transdiaphragmatic pressure of 34.3 Pa ($SE = 2.9$). The transdiaphragmatic ratios ranged from 1.86 to 1.16 (Table 1). ANOVA revealed significant ($F = 8.43$, $p = 6.0^{-7}$, $N = 6$) differences in the transdiaphragmatic ratios among the alligators. Post-hoc Bonferroni analysis confirmed the same scaling-related pattern of significant differences clustering in the comparisons between the smallest and largest alligators.

The ITP and IPP curves were typically synchronous and symmetrical (Figure 12a). Though uncommon, traces

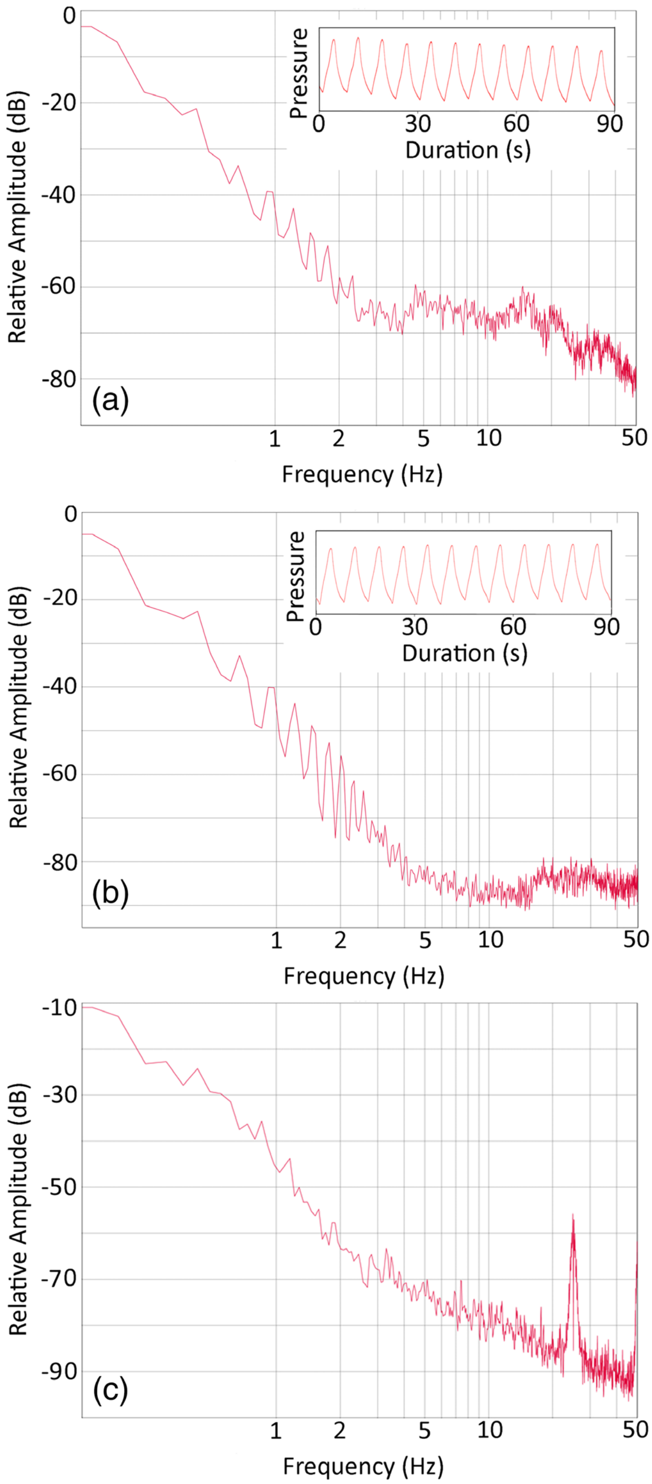

FIGURE 10 Power spectral analyses of the (a) intrathoracic pressure, (b) intraperitoneal pressure, and (c) exhalatory CO_2 all recorded simultaneously from a 178 cm *Alligator mississippiensis*. The raw pressure data traces are shown in the insets. Note that the Power Spectra show a dominant frequency (0.13 Hz) corresponding to the ventilatory frequency, and that the harmonics of this frequency (particularly evident from 1 to 2 Hz) are recovered from both pressure traces. The Power Spectrum from the exhalatory CO_2 lacks the clear harmonics, and has a prominent pump artifact at 25 Hz

were recorded in which the ITP or the IPP had a temporal offset from the other pulse curve (Figure 12c,d). Smaller pressure peaks were occasionally found between the ventilatory pulses (Figure 12b,c), primarily in the ITP traces.

3.3 | Visceral displacement

When the alligators were tilted 30° head-up, there was a rapid increase in IPP, and a corresponding decrease in ITP; the decrease in ITP was large enough to create negative pressures in the pleural cavities (Figure 13). During the head-up rotations the exhalatory CO_2 levels increased, and the ITP and IPP pulses increased in amplitude (Figure 13). Rotating the alligators into a 30° head-down posture resulted in a rapid drop in IPP, this drop was of magnitude to create negative pressures in the peritoneal cavity (Figure 14). The head-down rotation produced an increase in ITP (Figure 14). Exhalatory CO_2 levels decreased after head-down rotations, as did the amplitudes of the ITP and IPP pulsations.

Rotating the alligator produced significantly greater pressure changes in the peritoneal cavity than in the pleural cavity (Table 2), regardless of whether the rotations were head-up ($t = 3.31$, $p = .001$, $N = 13$) or head-down ($t = 3.19$, $p = .002$, $N = 13$). Setting aside the direction (negative or positive) of the pressure change, the magnitude of change was not significantly different between head-up and head-down rotations for either the IPP ($t = 0.307$, $p = .38$, $N = 13$) or the ITP ($t = 0.488$, $p = .31$, $N = 13$). Reflecting the similar magnitude of changes in the ITP and IPP, the transdiaphragmatic pressures were not significantly different between the head-up and head-down rotations ($t = 0.66$, $p = .26$, $N = 13$).

The ITP and IPP changed with rotation, as did the power spectral profile of the ITP and IPP pulsations. Figure 15 shows a power spectral analysis of the same alligator that was switched from a head-up to a head-down rotation within <4 min. Equal lengths of pulsations were analyzed for each power spectrum; these pulsations excluded the actual tilting transition period. Both the head-down and head-up rotations resulted in a shift of power spectral profile when compared to the horizontal levels (Figure 15). If the power spectra are compared, the head-down rotations amplified the low frequency (<1 Hz) vibrations of the PPS, while the head-up rotations damped those vibrations (Figure 15).

3.4 | Breaths

There were two, distinctly different, types of breaths recorded; hereafter these will be referred to asynchronous

TABLE 1 Summary of pressures, expressed in Pascals (mean, standard error) for the six specimens of *Alligator mississippiensis*, during stable horizontal ventilatory cycles

Body mass (kg)	Thoracic pressure	Peritoneal pressure	Paired *T* test	Transdiaphragmatic pressure (T–P)	Trasndiaphragmetic ratio (T/P)
7.9	157.9 (8.8)	89.0 (5.3)	$t = 9.46^{**}$, $N = 24$	64.6 (7.3)	1.86 (0.09)
11.3	156.2 (5.0)	94.8 (4.6)	$t=10.87^{**}$, $N=24$	61.5 (5.7)	1.73 (0.10)
11.8	147.6 (7.6)	112.1 (4.8)	$t = 4.25^{**}$, $N = 18$	35.5 (8.3)	1.35 (0.09)
12.9	70.3 (3.6)	46.9 (1.8)	$t = 6.83^{**}$, $N = 24$	23.4 (3.4)	1.53 (0.09)
16.3	37.7 (2.6)	34.1 (2.6)	$t = 1.94$, $N = 27$	3.6 (1.9)	1.16 (0.06)
23	63.5 (4.5)	49.1 (5.5)	$t = 3.85^{**}$, $N = 21$	17.5 (3.7)	1.43 (0.11)

Note: The paired *T* test compared the thoracic and peritoneal pressures during the same ventilatory cycle.

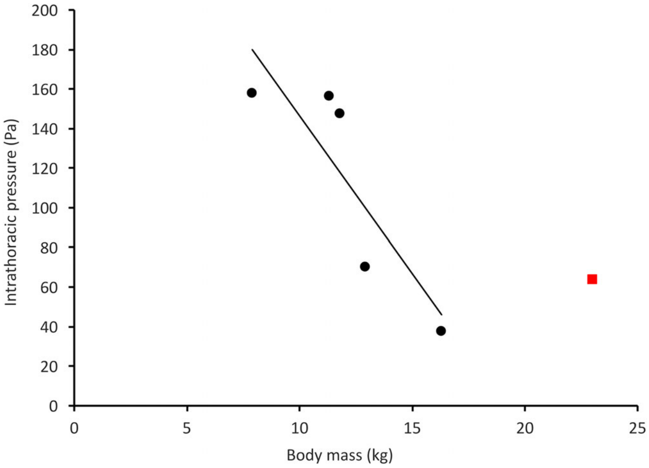

FIGURE 11 Plot of intrathoracic pressure (Y-axis in Pa) against alligator body mass (X-axis in kg). The five smaller specimens are indicated by black dots; the indicated linear regression line was based only on these five animals. The volume supplied in each pulse was increased for the largest alligator (red square) resulting in an increased intrathoracic pressure relative to the trend

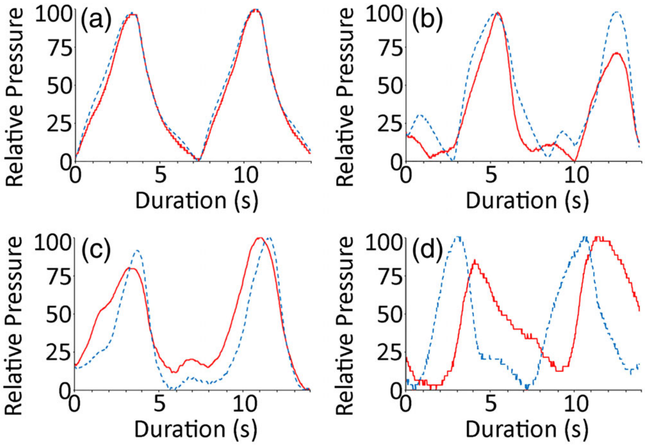

FIGURE 12 Variations in the intrathoracic (blue dashed) and intraperitoneal (red solid) pressure pulses. All of the pairs of pressure pulses represented in this figure were recorded simultaneously; no temporal alterations have been made. To emphasize the variations in the pulses, the range of each pulse has been mathematically adjusted so that each pair of pulses has the same minimum and maximum pressure level

and synchronous breaths. The asynchronous breaths always began with a spike in IPP, and a corresponding negative pulse in ITP (Figure 16a). As the spike in IPP began to decrease, there was a marked increase in ITP; this later ITP increase was typically of lower amplitude but longer duration (Figure 16a). The increase in ITP was never associated with negative levels of IPP. The synchronous breaths were marked by a gradual (not spiked) increase in both IPP and ITP, a decrease in both to near the baseline values, then (typically) a second increase (Figure 16b). Negative pressures were never observed during the synchronous breaths. The temporal and amplitude pattern of the ITP and IPP curves were not identical during synchronous breaths (Figure 16b), but the similar amplitudes, and nearly concurrent changes, in the two pressures made the synchronous breaths easy to distinguish from the asynchronous breaths.

While the basic distinction between synchronous and asynchronous breaths held across all the experimental trials, the breaths recorded demonstrated very high levels of variation, even within each alligator (Figure 17). This variation included both temporal and amplitude differences; in fact, no two recorded breaths were the same.

Comparing five synchronous and five asynchronous breaths pooled from multiple alligators (Table 3), demonstrates that the typical second pressure rise of the synchronous breaths makes these significantly ($t = 2.79$, $p = .011$) longer episodes than the asynchronous breaths. The peak ITP was significantly ($t = 2.47$, $p = .019$) higher in the synchronous breaths; the IPPs recorded from synchronous and asynchronous breaths were not significantly different ($t = 0.66$, $p = .26$). During the

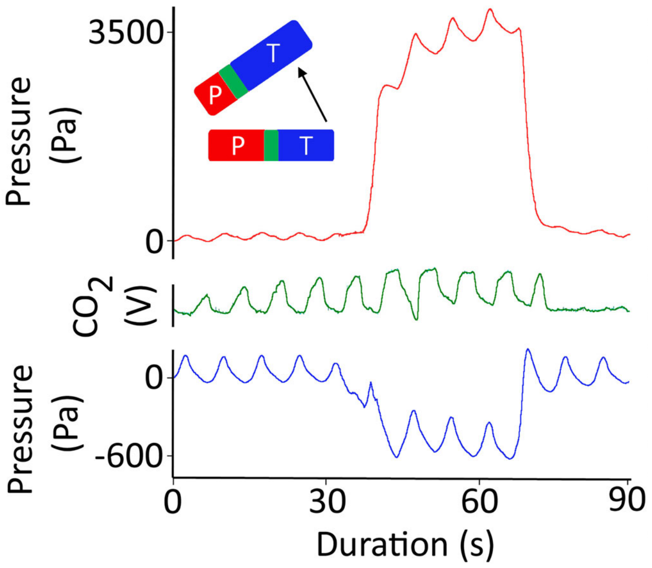

FIGURE 13 Date traces recorded during a head-up tilt of a 163 cm *Alligator mississippiensis*. The schematic insert depicts the hypothesized result of the tilt. The liver (green) and fused postpulmonary septum, would displace caudally decreasing the size of the peritoneal cavity (P) and increasing IPP, while increasing the size of the thoracic cavity (T) and decreasing ITP. Note that the scales of the Intraperitoneal pressure (top trace, red) and intrathoracic pressure (bottom trace, blue) are not the same. This head-up rotation resulted in increases in the pulsatile amplitude of the exhalatory CO_2 (middle trace, green), ITP, and IPP

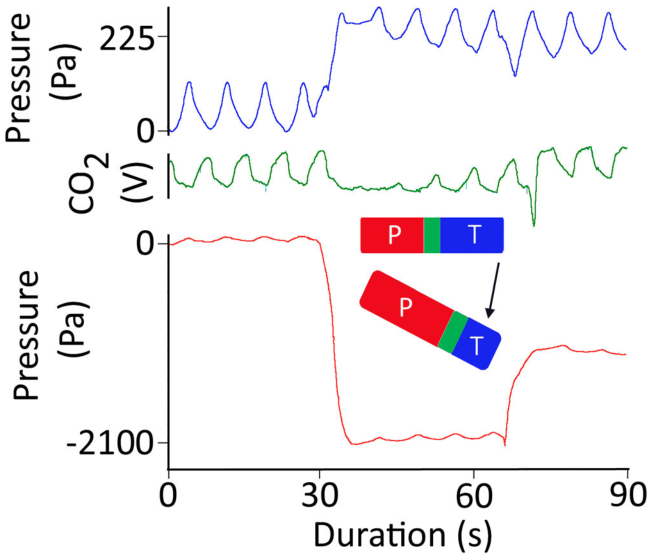

FIGURE 14 Date traces recorded during a head-down tilt of a 163 cm *Alligator mississippiensis*, recorded within 5 min of (Figure 13). The schematic insert depicts the hypothesized result of the tilt. The liver (green) and fused postpulmonary septum would displace cranially decreasing the size of the thoracic cavity (T) and increasing ITP, while increasing the size of the peritoneal cavity and decreasing IPP. Note that the scales of the Intraperitoneal pressure (bottom trace, red) and intrathoracic pressure (top trace, blue) are not the same. This head-down rotation resulted in decreases in the pulsatile amplitude of the exhalatory CO_2 (middle trace, green), ITP, and (slightly) IPP. This was an unusual rotation in that when the animal was returned to horizontal the data traces slowly returned to baseline; in a "typical" tilt the return to baseline produces more abrupt changes in the data traces (Figure 13), note that the "recovery" traces were never quantified

synchronous breaths the ITP and IPP shifted in unison, such that there were no significant differences between the two pressures ($t = 0.08$, $p = .47$). In the asynchronous breaths, the ITP and IPP spikes were separated temporally, and also differed significantly in amplitude ($t = 2.35$, $p = .023$).

As shown in Figure 18, these breaths could have a marked influence on the body cavity pressure. The trace shown in Figure 18, though demonstrative of these pressure changes, was excluded from analysis.

4 | DISCUSSION

As Perry (1998) noted, the intracoelomic partitions of reptiles have been relatively understudied, particularly in comparison to the structure of the lungs or ventilatory mechanics. Duncker (1978a) provided a detailed description of the postpulmonary septum of *Caiman crocodilus*. The only discrepancy with the current work is that Duncker (1978a) noted that the lateral margin of the postpulmonary septum was "well-developed sliding connective tissue" (gutausgebildetes Verschiebebindegewebe, translation Prof. Young). Duncker (1978a) did not perform histological analyses; this well-developed connective tissue is what is shown in the present contribution to have a core of smooth muscle. Our schematic summary figure of *Alligator mississippiensis* (Figure 8) can be easily aligned with the summary figure presented by Duncker (1978b) and later by Perry (1998). Van der Merwe and Kotze (1993) have provided a more recent description of the diaphragm in a crocodilian (*Crocodylus niloticus*); the key features they described are similar to what is reported herein for *A. mississippiensis*.

The numerous attachments that are present between the visceral pleura of the Crocodylian lung and the parietal or mediastinal pleura have been detailed (Duncker, 1978b; Perry, 1985, 1988, 1998); these attachments (which are outside of the scope of this contribution) are referred to as pulmonary ligaments, mesopneumonia, or simply attachments. These connections are numerous enough that Perry (1988) hypothesized that the Crocodylian lung had a static relationship with the thoracic wall and surrounding viscera; essentially that the lung would expand and deflate but not be

TABLE 2 Body cavity pressures in *Alligator mississippiensis* (expressed in Pascals as mean, standard error) during 30° head-up or head-down tilts

	Intrathoracic pressure	Intraperitoneal pressure	Transdiaphragmatic pressure (T-P)	Transdiaphragmatic pressure (T/P)
Head-down rotation	1621.7 (260.5)	−4384.1 (823.1)	6005.7 (1063.2)	−0.39 (0.02)
Head-up rotation	−1350.8 (296.4)	4042.9 (742.8)	−5393.7 (986.7)	−0.36 (0.06)

physically displaced during ventilation. Farmer (2015) has described the intrathoracic cavity of Crocodylians, and Claessens (2009) demonstrated that this space is dynamic, not static. It is this dynamic intrathoracic cavity that was recorded from in this study.

The experimental approach to recording intrathoracic (ITP) and intraperitoneal pressures (IPP) used in this study is unconventional. Though the differential pressure transducers used in this study were designed to measure ITP and IPP, they are normally connected to esophageal catheters (e.g., Pavlidou, Savvas, Moens, Vasilakos, & Raptopoulos, 2013; Slocombe, Brock, Covelli, & Bayly, 1991). The decision to not use esophageal catheters on *A. mississippiensis* was based on several considerations: the mammalian diaphragm is much thicker than the Crocodylian PPS, the mammalian stomach is more isolated from the pleural cavity than it is in Crocodylians, physical displacement of the stomach could interfere with the catheter, and one of the objectives of this study was to directly record PPS vibration, which would not be possible with an esophageal catheter. Previous studies have implanted balloon catheters into the thoracic or peritoneal cavities (e.g., Pinsky, Matuschak, & Klain, 1985); but this approach seemed incompatible with the visceral displacements that were designed into this study.

As noted earlier, these experiments were not intended to explore Crocodylian ventilation, or airflow within the lung of *Alligator mississippiensis*. Exhalatory CO_2 was used as a marker of the airflow cycle; no attempt was made to recreate the natural unidirectional pattern of airflow through the lung (Farmer & Sanders, 2010). Farmer (2010) detailed a cardiogenic influence on airflow through the Crocodylian lung; the bi-directional ventilatory system used in this study may have disrupted these cardiogenic airflow dynamics.

The resting (baseline) levels of ITP and IPP recorded differed from the typical mammalian pattern in that the ITP was consistently slightly positive and the ITP was consistently slightly negative. Presumably this is artefactual. Having an anesthetized animal (so no abdominal skeletal muscle support) in a prone position may have caused slight cranial displacement of the viscera due simply to the animal's body mass. This displacement could cause a slight decrease in IPP and a slight increase in ITP.

The pulmonary inflation performed was designed to cause repeated slight expansion of the lungs, and with this, cyclic changes in the ITP. Note that while the pressure curves presented herein are similar in appearance to those given by Boelaert (1942) in his study on ventilation in *A. mississippiensis*, Boelaert recorded voluntary lateral expansion of the abdominal and thoracic body walls, while this study recorded the pressures within these cavities. This study was designed to minimize/avoid the type of body wall expansion that Boelaert (1942) documented. The strong temporal correlation between exhalatory CO_2 and ITP (Figure 9), the negative regression between specimen body mass and ITP (Figure 11), and the fact that the ventilatory frequency is the dominant frequency in the power spectrum of the ITP (Figure 10), all support the conclusion that the pulsations recorded from the intrathoracic cavity (the ITP) were caused by the mechanical ventilation provided to the anesthetized *A. mississippiensis*. Power spectral analysis of the ITP curves (Figure 10) show a dominant frequency that corresponds to the mechanical ventilation rate (0.13 Hz), as well as harmonics of this frequency. The ITP power spectrum is distinct from the power spectrum of the exhalatory CO_2 (Figure 10), indicating that the vibrations evident in the ITP power spectrum are not originating from the lung. Within the pleural cavity there would appear to be two likely candidates for these pressure-induced vibrations, the mediastinum or the PPS (Figure 4).

The Intraperitoneal pressure recordings (IPP) visually paralleled the ITP traces (Figure 9). The IPP had significantly lower amplitude than the ITP, thus the transdiaphragmatic pressures (mean of 34.3 Pa) were significantly >0 (Table 1). Spectral analysis of the IPP traces revealed the same dominant frequency and harmonics that were recovered from the ITP (Figure 11).

The significant transdiaphragmatic pressures indicate that the PPS of *Alligator mississippiensis* is capable of

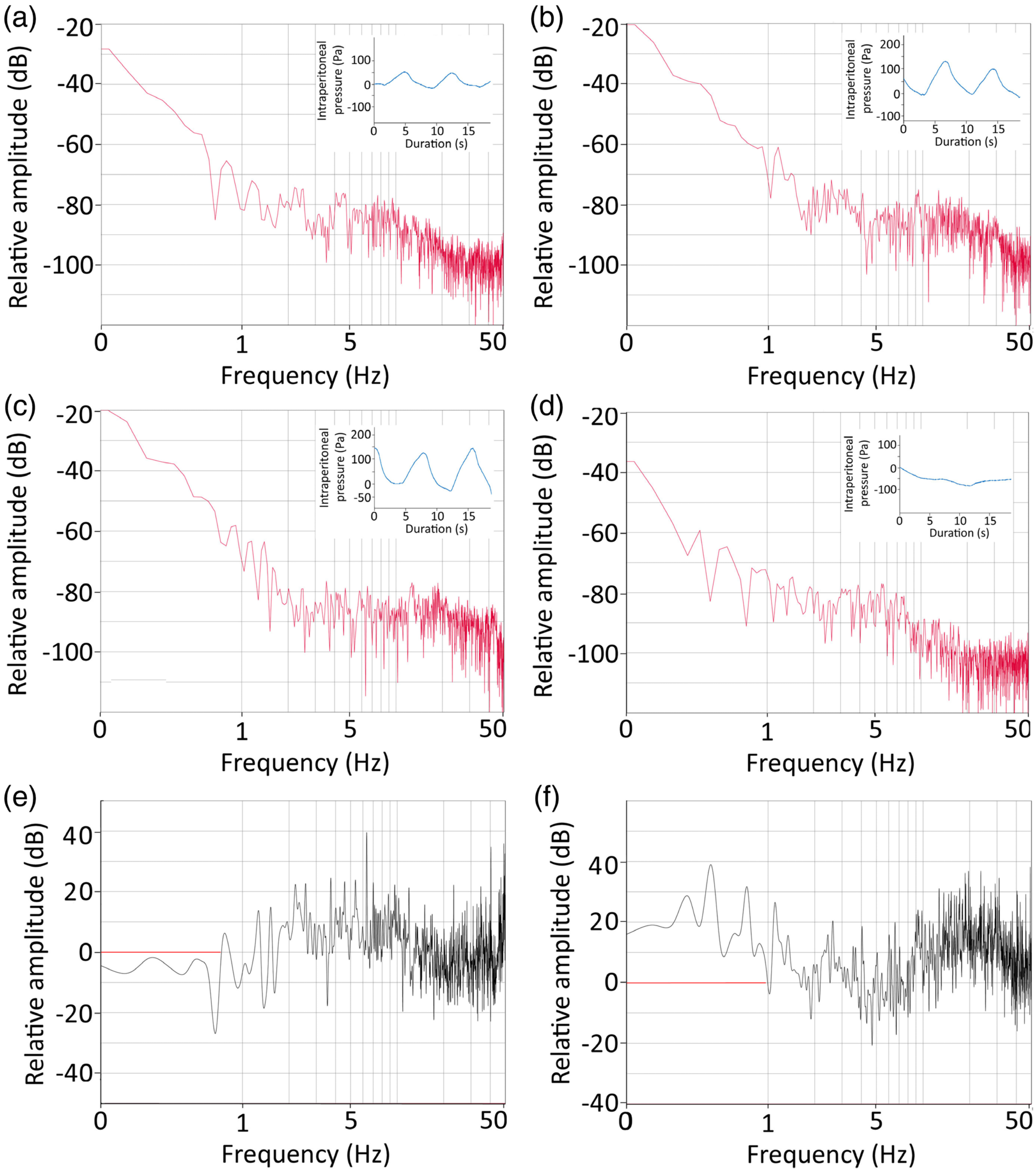

FIGURE 15 Power spectral analyses of the IPP pulses recorded from the same 188 cm *Alligator mississippiensis* during head-up (left; a,c,e) and head-down (right; b,d,f) rotations. These power spectral analyses are based on the same length of pressure pulse data (insets) recorded immediately before (a,b) or after (c,d) the rotation; the brief transition period was not analyzed. The power spectra of both postrotation (c,d) traces differ from the respective prerotation traces (a,b). If the prerotation power spectra (a,b) are subtracted from the postrotation (c,d) power spectra, the composite spectra for head-up (e) or head-down (f) rotations are produced; note that these two composites are almost mirror images of each other in terms of the frequency power distribution relative to 0 (red line)

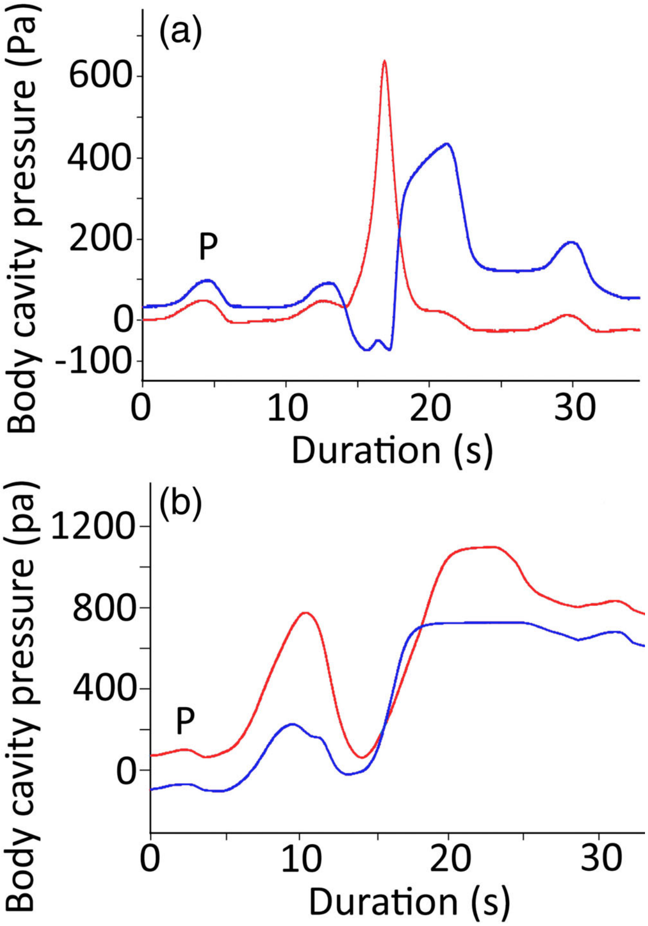

FIGURE 16 Data traces of the IPP (red) and ITP (blue) during an (a) asynchronous and (b) synchronous breath. In both graphs the data tracings are shown at the same scale, and one prebreath ventilator pulse (P) is shown for reference. Note the clear initial negative ITP pressure that characterizes the asynchronous breaths (a), and the long durations of these breaths, particularly the synchronous variety (b)

functionally separating the pleural and the peritoneal cavities. Given that there are two separate cavities, but the pressure traces within them reveal the same power spectrum, and that the mediastinum is not continued into the peritoneum, the power spectra of the ITP and the IPP are interpreted as the vibratory signature of the PPS of *A. mississippiensis*.

It is worth emphasizing that when proposing that the PPS of the *A. mississipiensis* vibrates, it is not meant that the PPS is an independent free-standing sheet in the body cavity. The PPS has varying degrees of fusion to the liver, the pericardial sac, the lungs, the stomach, and is attached to the inner surface of the body wall all along its perimeter (Figure 5). There would seem to be limited potential for the PPS to vibrate in these regions. But as shown in Figure 4, the PPS has a dorsal portion that is not fused to other viscera, and on the dorsolateral portions the PPS has the extending hepatopulmonary bursae, which are similarly not fused to other viscera. Having vibrations restricted to localized portions of the PPS could also explain the occasional presence of some asymmetry between the ITP and IPP traces (Figure 12).

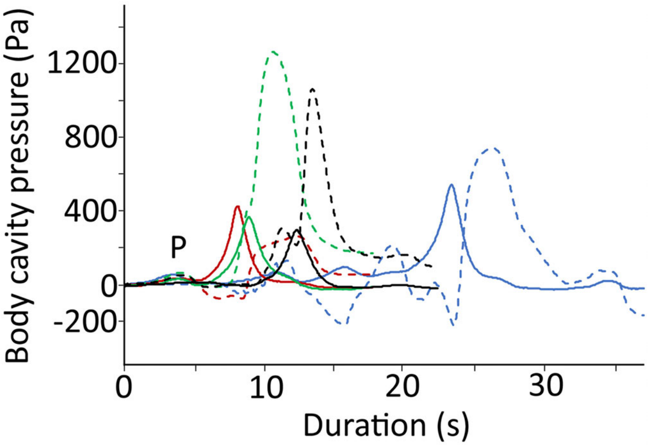

FIGURE 17 Example of the temporal and amplitude variation in the breaths recorded from *Alligator mississippiensis*. All of these breaths were recorded from the same individual. The pressure changes during four breaths are shown, with an initial ventilator pulse (P) for reference; all four breaths are shown at the same scale. The breaths are color coded with ITP shown by dashed lines and IPP shown by solid lines. These breaths include two synchronous breaths (green and black traces), one asynchronous breath (red trace) and an unusual breath that appears to be two successive asynchronous breaths (blue trace)

The transdiaphragmatic pressures obtained from *Alligator mississippiensis* during the pulmonary inflation trials are much lower than what has been reported from humans (15.5 MPa, Laporta & Grassino, 1985) and other mammals (e.g., 2 MPa in walking horses, Ainsworth et al., 1996; 1 MPa in mice, Greising, Sieck, Sieck, & Mantilla, 2013). The mammalian transdiaphragmatic pressures are much higher, in part, because they are recorded from naturally ventilating subjects, as opposed to the minimal lung pulsations used in this study. The difference in magnitude also stems, in part, from the increased thickness and structural integrity of the mammalian diaphragm.

The visceral displacement (tilting) experiments were designed to exploit the known mobility of the crocodilian liver (e.g., Gans & Clark, 1976). These trials involved 30° rotations on the assumption that this was adequate to displace the liver, without causing physiological risk to the animal (Knoche, Young, & Kondrashova, 2019; Kondrashova, Blanchard, Knoche, Potter, & Young, 2020). The displacement of the viscera was not monitored; however, the fact that every rotation resulted in a rapid change in both ITP and IPP strongly suggests

TABLE 3 Maximum body cavity pressures (expressed in Pascals as mean, standard error) recorded from *Alligator mississippiensis* performing voluntary "breaths"

	Duration	Number of pulses	Intrathoracic pressure max	Intraperitoneal pressure max
Synchronous	18.5, 2.5	2	816.7, 192	798.2, 147.7
Asynchronous	11.1, 0.8	1	316.1, 65.6	1178.6, 112.3

Note: The duration is given in seconds, number of pulses refers to discrete pressure increases per "breath."

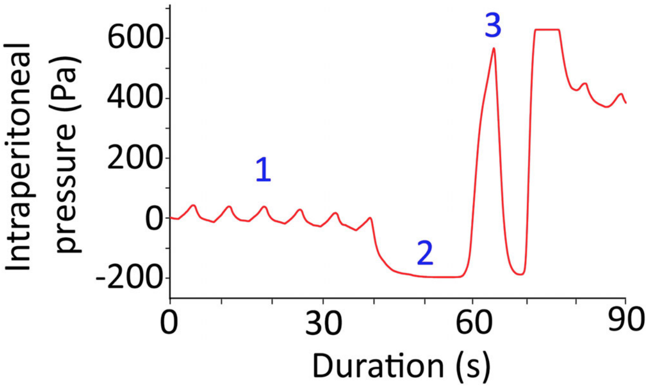

FIGURE 18 Changes in the IPP of a 143 cm *Alligator mississippiensis* during ventilatory pulsations (1), a head-down rotation (2), and what appears to be an asynchronous breath (3). The termination of the breath coincided with the return of the animal to horizontal, so the influence of those two events could not be distinguished. During this recording the visceral shift associated with the head-down rotation displaced the thoracic pressure sensor slightly, which disrupted the corresponding ITP data trace

that the viscera were moving. There were three key results from the visceral displacement trials: 1) the pressure changes were as predicted for liver displacement; 2) the direction of pressure change in the ITP was always opposite that of the IPP; and 3) the pressures were maintained until the animal was returned to the horizontal (Figures 13 and 14). The ability of the tilts to establish opposite (negative vs. positive) pressures in the pleural and peritoneal cavities, which were maintained throughout the tilt, is only possible if the PPS is functionally separating the two cavities. Power spectral comparisons between the baseline (horizontal) and rotated IPP traces show opposite shifts in the power spectral density (Figure 15) when comparing head-up and head-down rotations from the same animal. These differences are taken as reflecting changes in the tensile state of the PPS caused by the visceral displacement.

The pressures recorded during the visceral displacement were significantly higher than those recorded during the pulmonary inflation trials (Table 2); the rotation trials were also marked by higher levels of variation. Some of this variation is likely intrinsic. As evident in Figure 3, the stomach of these captive *Alligator mississippiensis* retained a great deal of rat hair and partially digested rats. Presumably differential levels of gastric expansion could influence liver mobility.

Two different patterns of "breaths" were recorded. The asynchronous breaths (Figure 16a) are interpreted as *A. mississippiensis* contracting the diaphragmaticus muscle and displacing the liver caudally, causing a sharp increase in IPP and a corresponding drop in ITP. The "second part" of the asynchronous breath is the sharp decrease in IPP which is associated with the more gradual increase in ITP; this is assumed to represent the return of the liver to the original position, but the mechanism of this return is not clear from the pressure traces.

The synchronous breaths (Figure 16b) do not appear to involve the diaphragmaticus muscle, but rather active contraction of the thoracic and abdominal body wall muscles. Since the animal was actively compressing both the thoracic and peritoneal body cavities, the only evidence for a functional PPS in these traces is the (varying) difference in positive ITP and IPP pressures. During normal ventilation *A. mississippiensis* may use varying patterns of body wall contraction (Farmer & Carrier, 2000b); the same variation was evident in the diversity of the synchronous "breaths" recorded from the anesthetized animals (Figure 17).

This study provides anatomical evidence for the presence of a PPS that spans the entire body cavity in *Alligator mississippiensis*. Pressure recordings from the intrathoracic and intraperitoneal cavities reveal that the PPS is capable of maintaining separate (significantly different) pressures within the two body cavities, and that the integrity of the PPS is not disrupted by what was interpreted as either induced or voluntary displacements of the liver. Power spectral analyses suggest that portions of the PPS can vibrate; experimentally induced changes to the power spectral density further suggest that the PPS is not static but rather is capable of dynamic changes in tension.

Recognition of the dynamic nature of the PPS is important, particularly in light of the smooth muscle that is present in portions of the PPS. Van der Merwe and Kotze (1993) state that the ventral third of the PPS of *Crocodylus niloticus* is "muscular." In *Alligator mississippiensis* the PPS includes smooth, not skeletal, muscle (Figure 7); this smooth muscle is most prominent in the lateral and ventral portions of the PPS and is organized into bands of smooth muscle fibers that course medio-laterally. The presence of these smooth muscle bands is taken as evidence that *A. mississippiensis*, and presumably all Crocodylians, can actively contract, and thereby adjust or tune, their PPS.

Histological analysis (Figure 5) and even gross dissection (Figure 6) demonstrates that the PPS is a distinct structure from the capsule of the liver, notwithstanding the fact that the caudal surface of the PPS has extensive fusion with the cranial surface of the liver capsule. This distinction is not always clear in the literature. The diaphragmaticus muscle has been described as forming a skeletal muscle diaphragm, and as inserting (or integrating) into the PPS (e.g., Klein & Owerkowicz, 2006); neither of these claims seem technically correct, at least in regards to *A. mississippiensis*.

More importantly than identifying the connective tissue layers, is the recognition that in crocodilians there are three active mechanisms for "tuning" the PPS. One mechanism is the contraction of the diaphragmaticus which can displace the liver and, through the fusion between the liver capsule and the PPS, alter the tensile state and/or physically displace, the PPS. The second mechanism is the contraction of the smooth muscle fibers that are intrinsic to the PPS which can physically displace, and/or alter the tensile state of, the PPS. The third mechanism is through abduction or adduction of the ribs and lateral body wall. The diaphragmaticus can be simplified as having a caudal line of action (e.g, Gans & Clark, 1976). The intrinsic muscle of the PPS, and the displacement of the body wall, would have a lateral line of action; since the diaphragmaticus is caudal to the PPS, these skeletal and smooth muscle forces are antagonistic.

The results presented herein suggest that the PPS of *Alligator mississippiensis* can influence ventilation; indeed, some of the transdiaphragmatic pressures we recorded during tilts and breaths (Tables 2 and 3) exceed those reported from some mammals. Our experiments focused on the potential role of the PPS during ventilation because of the experimental accessibility of the ventilatory mechanics. As previous workers (e.g., Perry et al., 2010) have detailed, a diaphragm can perform a variety of nonventilatory functions. We have no basis to assume that the PPS of *A. mississippiensis* exclusively, or even primarily, functions in ventilation. The functional links between the liver, the PPS, and the ITP and IPP levels, suggest that the PPS may play a functional role in buoyancy control (Uriona & Farmer, 2008).

This study was motivated, in part, by the work of Klein and Owerkowicz (2006) who summarized the diversity of intracoelomic septa, and sparked our curiosity by the use of the term "proto-diaphragm." The postpulmonary septum of Crocodylians, like the mammalian diaphragm develops, from the transverse septum (e.g., Hochstetter, 1906); this supports the hypothesis that the two may be homologous structures (Klein & Owerkowicz, 2006). The postpulmonary septum of *A. mississippiensis* is muscular, dynamic, and capable of maintaining a trans-diaphragmatic pressure. In these, and likely other respects, the postpulmonary septum of *A. mississippiensis* is analogous to the mammalian diaphragm. Accordingly, it seems fully justified, and arguably more accurate, to refer to the postpulmonary septum of *A. mississippiensis* as a diaphragm.

ACKNOWLEDGMENTS

The authors wish to thank Ruth Elsey and the Louisiana Wildlife and Fisheries Department. Portions of this research were supported by an internal A.T. Still University research award (Warner/Fermaturo) to Prof. Young. The authors thank Peter Kondrashov for his continued support.

AUTHOR CONTRIBUTIONS

Michael Cramberg: Data curation; formal analysis; investigation; methodology; supervision; validation; visualization; writing-review & editing. **Skye Greer:** Formal analysis; investigation; methodology; validation; visualization; writing-review & editing. **Bruce Young:** Conceptualization; data curation; formal analysis; investigation; methodology; project administration; resources; supervision; validation; visualization; writing-original draft; writing-review & editing.

ORCID

Bruce A. Young https://orcid.org/0000-0002-0988-7731

REFERENCES

Agostoni, E., & Rahn, H. (1960). Abdominal and thoracic pressures at different lung volumes. *Journal of Applied Physiology*, *15*, 1087–1092.

Ainsworth, D., Eicker, S., Nalevanko, M., Ducharme, N., Hackett, R., & Snedden, K. (1996). The effect of exercise on diaphragmatic activation in horses. *Respiration Physiology*, *106*, 35–46.

Axelsson, M., Franklin, C. E., Lofman, C. O., Nilsson, S., & Grigg, G. C. (1996). Dynamic anatomical study of cardiac shunting in crocodiles using high-resolution angioscopy. *The Journal of Experimental Biology*, *199*, 359–365.

Bishop, B. (1963). Abdominal muscle and diaphragm activities and cavity pressures in pressure breathing. *Journal of Applied Physiology*, *18*, 37–42.

Boelaert, R. (1942). Sur la physiologie de la respiration de l' *Alligator mississipiensis*. *Archives Internationales de Physiologie*, *52*, 57–72.

Brocklehurst, R., Moritz, S., Codd, J., Sellers, W., & Brainerd, E. (2017). Rib kinematics during lung ventilation in the American alligator (*Alligator mississippiensis*): An XROMM analysis. *The Journal of Experimental Biology*, *220*, 3181–3190.

Brocklehurst, R., Schachner, E., Codd, J., & Sellers, W. (2020). Respiratory evolution in archosaurs. *Philosophical Transactions of the Royal Society B*, *375*, 20190140.

Butler, G. (1889). On the subdivision of the body-cavity in lizards, crocodiles, and birds. *Proceedings of the Zoological Society of London*, *1889*, 452–474.

Claessens, L. (2009). A cineradiographic study of lung ventilation in *Alligator mississippiensis*. *The Journal of Experimental Zoology*, *311A*, 1679–1687.

Douse, M., & Mitchell, G. (1992). Episodic breathing in alligators: Role of sensory feedback. *Respiration Physiology*, *87*, 77–90.

Duncker, H. (1978a). Coelom-Gliederung der Wilbeltiere: Funktionelle Aspekte. *Verhandlungen der Anatomischen Gesellschaft*, *72*, 91–112.

Duncker H. 1978b. Funktionsmorphologie des Atemapparates und Coelomgliederung bei Reptilien, Vogeln und Saugetieren. *Verhandlungen der deutschen Zoologischen Gesellschaft 1978*: 99–132.

Duncker, H. (1979). Coelomic cavities. In A. King & J. Mclelland (Eds.), *Form and function in birds* (Vol. 1, pp. 39–67). London: Academic Press.

Farmer, C. (2010). The provenance of alveolar and parabronchial lungs: Insights from paleoecology and the discovery of cardiogenic, unidirectional airflow in the American alligator (*Alligator mississippiensis*). *Physiological and Biochemical Zoology*, *83*, 561–575.

Farmer, C. (2015). Similarity of crocodilian and avian lungs indicate unidirectional flow is ancestral for archosaurs. *Integrative and Comparative Biology*, *55*, 962–971.

Farmer, C., & Carrier, D. (2000a). Pelvic aspiration in the American alligator (*Alligator mississippiensis*). *The Journal of Experimental Biology*, *203*, 1679–1687.

Farmer, C., & Carrier, D. (2000b). Ventilation and gas exchange during treadmill locomotion in the American alligator (*Alligator mississippiensis*). *The Journal of Experimental Biology*, *203*, 1671–1678.

Farmer, C., & Sanders, K. (2010). Unidirectional airflow in the lungs of alligators. *Science*, *327*, 338–340.

Gans, C., & Clark, B. (1976). Studies on ventilation of *Caiman crocodilus* (Crocodilia:Reptilia). *Respiration Physiology*, *26*, 285–301.

George, J., & Shah, R. (1954). The occurrence of a striated outer muscular sheath in the lungs of *Lissemys punctata granosa* Schoepff. *Journal of Animal Morphology and Physiology*, *1*, 13–16.

Greising, S., Sieck, D., Sieck, G., & Mantilla, C. (2013). Novel method for transdiaphragmatic pressure measurements in mice. *Respiratory Physiology & Neurobiology*, *188*, 56–59.

Hochstetter, F. (1906). Uber die Entwicklung der Scheidewandbildungen in der Leibeshohle der Krokodile. In A. Voelzkow (Ed.), *Reise in Ostafrika* (Vol. 4, pp. 141–205). Stuttgart: Schweizbartsche.

Hodges, P., Butler, J., McKenzie, D., & Gandevia, S. (1997). Contraction of the human diaphragm during rapid postural adjustments. *The Journal of Physiology*, *505*, 539–548.

Hubmayr, R., Sprung, J., & Nelson, S. (1990). Determinants of transdiaphragmatic pressure in dogs. *Journal of Applied Physiology*, *69*, 2050–2056.

Klassen, M., Adams, J., Cramberg, M., Knoche, L., & Young, B. A. (2020). The narial musculature of *Alligator mississippiensis*: Can a muscle be its own antagonist? *Journal of Morphology*, *281*, 608–619. https://doi.org/10.1002/jmor.21124

Klein, W., & Owerkowicz, T. (2006). Function of intercoelomic septa in lung ventilation of amniotes: Lessons from lizards. *Physiological and Biochemical Zoology*, *79*, 1019–1032.

Klein, W., Bohme, W., & Perry, S. (2000). The mesopneumonia and post-hepatic septum of the Teiioidea (Reptilia:Squamata). *Acta Zoologica*, *81*, 109–119.

Klein, W., Abe, A., & Perry, S. (2003). Static lung compliance and body pressures in *Tupinambis merianae* with and without post-hepatic septum. *Respiratory Physiology & Neurobiology*, *135*, 73–86.

Klein, W., Andrade, D., Abe, A., & Perry, S. (2003a). Role of the post-hepatic septum on breathing during locomotion in *Tupinambis merianae* (Reptilia:Teiidae). *The Journal of Experimental Biology*, *206*, 2135–2143.

Klein, W., Andrade, D., Abe, A., & Perry, S. (2003b). Structure of the post-hepatic septum and its influence on visceral topology in the tegu lizard, *Tupinambis merianae* (Teiidae:Reptilia). *Journal of Morphology*, *258*, 151–157.

Knoche, L., Young, B. A., & Kondrashova, T. (2019). The influence of gravitational gradients on the American alligator (*Alligator mississippiensis*). *Anatomical and Physiological Current Research*, *9*, 318.

Kondrashova, T., Blanchard, J., Knoche, L., Potter, J., & Young, B. A. (2020). Intracranial pressure of the American alligator (*Alligator mississippiensis*): Reptilian meninges and orthostatic gradients. *Journal of Comparative Physiology A*. *206*, 45–54. https://doi.org/10.1007/s00359-019-01386-6

Laporta, D., & Grassino, A. (1985). Assessment of transdiaphragmatic pressure in humans. *Journal of Applied Physiology*, *58*, 1469–1476.

Lessa, T., de Abreu, D., Bertassoli, B., & Ambrosio, C. (2016). Diaphragm: A vital respiratory muscle in mammals. *Annals of Anatomy*, *205*, 122–127.

Lillie, M., Vogl, A., Raverty, S., Haulena, M., McLellan, W., Stenson, G., & Shadwick, R. (2017). Controlling thoracic pressures in cetaceans during a breath-hold dive: Importance of the diaphragm. *The Journal of Experimental Biology*, *220*, 3464–3477.

Lyson, T., Schachner, E., Botha-Brink, J., Scheyer, T., Lambertz, M., Bever, G., & de Queiroz, K. (2014). Origins of the unique ventilatory apparatus of turtles. *Nature Communications*, *5*, 5211.

Milsom, W. (1991). Intermittent breathing in vertebrates. *Annual Review of Physiology*, *53*, 87–105.

Munns, S., Owerkowicz, T., Andrewartha, S., & Frappell, P. (2012). The accessory role of the diaphragmaticus muscle in lung ventilation in the estuarine crocodile *Crocodylus porosus*. *The Journal of Experimental Biology*, *215*, 845–852.

Mushonga, B., & Horowitz, A. (1996). Serous cavities of the Nile crocodile (*Crocodylus niloticus*). *Journal of Zoo and Wildlife Medicine*, *27*, 170–179.

Pavlidou, K., Savvas, I., Moens, Y., Vasilakos, D., & Raptopoulos, D. (2013). The effect of four anesthetic protocols for maintenance of anaesthesia on trans-diaphragmatic pressure in dogs. *PLoS One*, *8*, e75341. https://doi.org/10.1371/journal.pone.0075341

Pelosi, P., Quintel, M., & Malbrain, M. (2007). Effect of intra-abdominal pressure on respiratory mechanics. *Acta Clinica Belgica*, *62*, 78–88.

Perry, S. (1985). Functional anatomy of the chest wall: Evolutionary aspects. In C. Roussos & P. Macklem (Eds.), *The thorax*. New York: M. Dekker.

Perry, S. (1988). Functional morphology of the lungs of the Nile crocodile, *Crocodylus niloticus*: Non-respiratory parameters. *The Journal of Experimental Biology*, *134*, 99–117.

Perry, S. (1998). Lungs: Comparative anatomy, functional morphology, and evolution. In C. Gans & A. Gaunt (Eds.), *Biology of the Reptilia* (Vol. 19, pp. 1–92). Society for the Study of Amphibians and Reptiles: Ithaca, New York.

Perry, S., Similowski, T., Klein, W., & Codd, J. (2010). The evolutionary origin of the mammalian diaphragm. *Respiratory Physiology & Neurobiology*, *171*, 1–16.

Pinsky, M., Matuschak, G., & Klain, M. (1985). Determinants of cardiac augmentation by elevations in intrathoracic pressure. *Journal of Applied Physiology*, *58*, 1189–1198.

Reichert, M., Oliveira, P., Souza, G., Moranza, H., Restan, W., Abe, A., & Milsom, W. (2019). The respiratory mechanics of the yacare caiman (*Caiman yacare*). *The Journal of Experimental Biology*, *222*, 1–11. https://doi.org/10.1242/jeb.193037

Sanchez, N., Tenofsky, P., Dort, J., Shen, L., Helmer, S., & Smith, R. (2001). What is normal intra-abdominal pressure? *The American Surgeon*, *67*, 243–248.

Slocombe, R., Brock, K., Covelli, G., & Bayly, W. (1991). Effect of treadmill exercise on intrapleural, transdiaphragmatic and intraabdominal pressures in standardbred horses. *Equine Exercise Physiology*, *3*, 83–91.

Syme, D. A., Gamperl, K., & Jones, D. (2002). Delayed depolarization of the cog-wheel valve and pulmonary-to-systemic shunting in alligators. *The Journal of Experimental Biology*, *205*, 1843–1851.

Uriona, T., & Farmer, C. (2006). Contribution of the diaphragmaticus muscle to vital capacity in fasting and postprandial American alligators (*Alligator mississippiensis*). *The Journal of Experimental Biology*, *209*, 4313–4318.

Uriona, T., & Farmer, C. (2008). Recruitment of the diaphragmaticus, ishiopubis and other respiratory muscles to control pitch and roll in the American alligator (*Alligator mississippiensis*). *The Journal of Experimental Biology*, *211*, 1141–1147.

van der Merwe, N., & Kotze, S. (1993). The topgraphy of the thoracic and abdominal organs of the Nile crocodile (*Crocodylus niloticus*). *The Onderstepoort Journal of Veterinary Research*, *60*, 219–222.

How to cite this article: Cramberg, M., Greer, S., & Young, B. A. (2022). The functional morphology of the postpulmonary septum of the American alligator (*Alligator mississippiensis*). *The Anatomical Record*, *305*(10), 3055–3074. https://doi.org/10.1002/ar.24692